Supplement of Earth Syst. Sci. Data, 16, 3893–3911, 2024
https://doi.org/10.5194/essd-16-3893-2024-supplement


*Supplement of*

# Monsoon Asia Rice Calendar (MARC): a gridded rice calendar in monsoon Asia based on Sentinel-1 and Sentinel-2 images

**Xin Zhao et al.**

*Correspondence to:* Xin Zhao (zhao.xin@nies.go.jp) and Kazuya Nishina (nishina.kazuya@nies.go.jp)

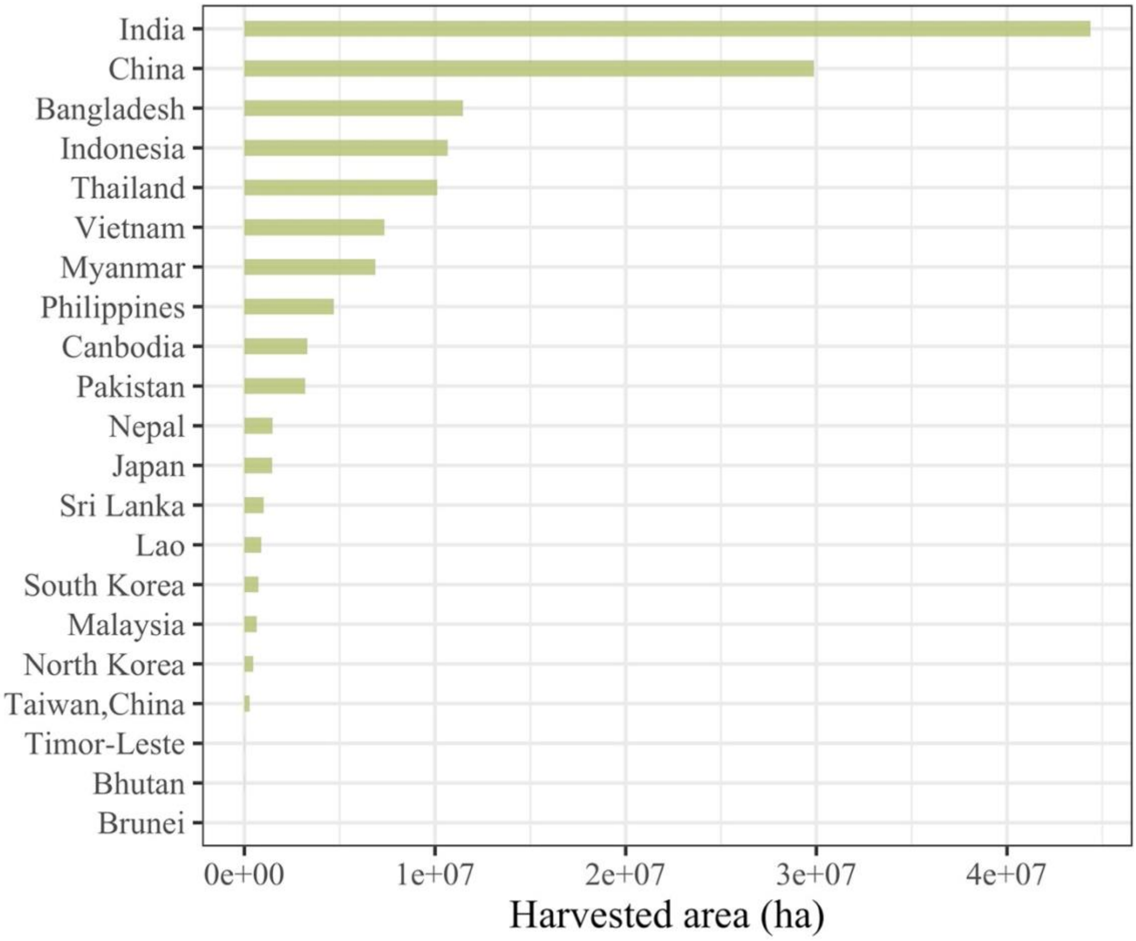


**Figure S1.** Harvested area of rice paddy fields for countries in monsoon Asia in 2019 and 2020. The data in this figure was derived from FAOSTAT (https://www.fao.org/faostat/en/#data) with last update on December 23, 2022 and access on 1 January 2023.

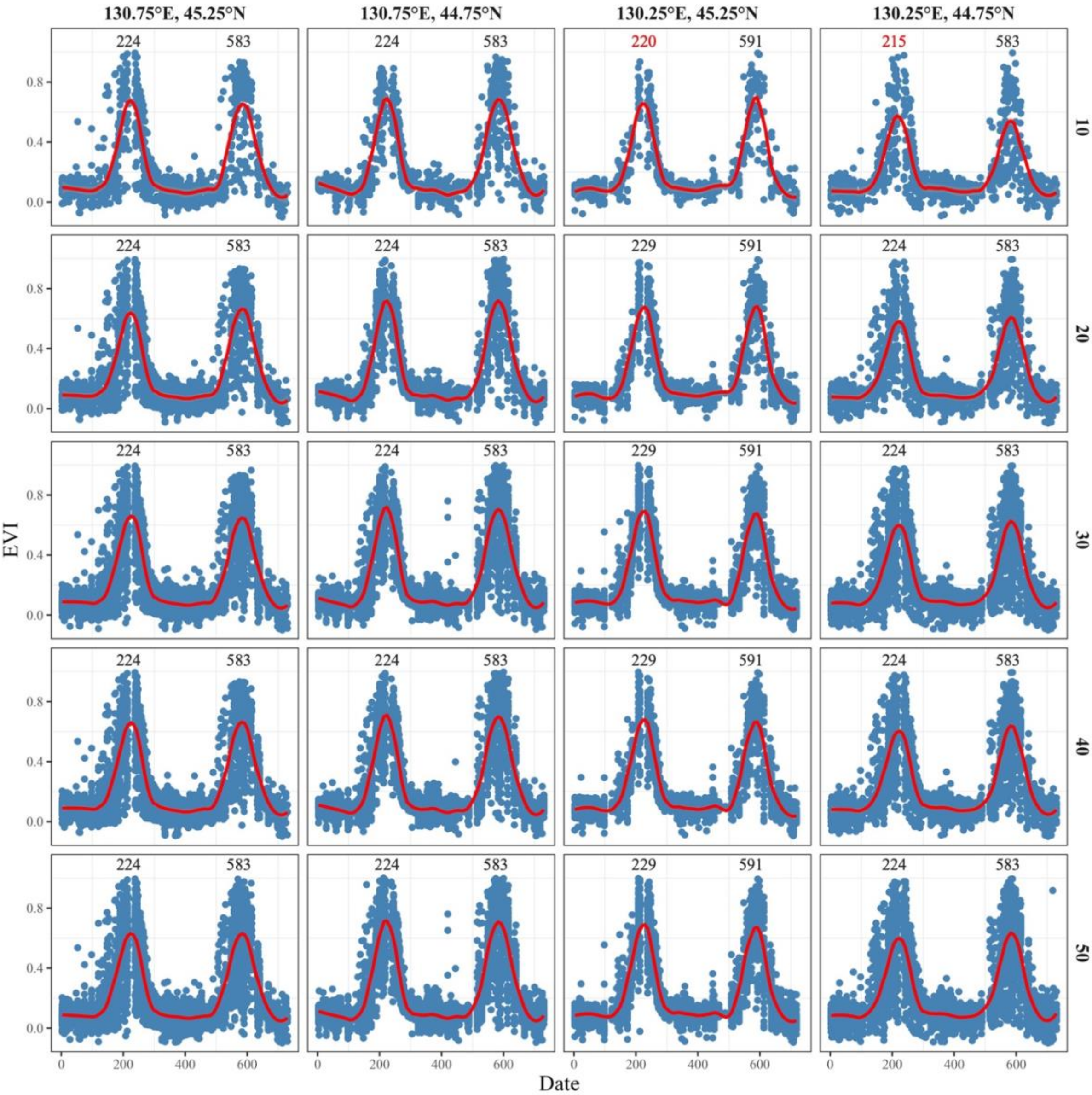


**Figure S2.** Example of the effect of sampling numbers in rice paddy fields (10, 20, 30, 40, and 50) for extracting phenological dates. X-axis denotes the days from 1 January 2019 to 31 December 2020, and Y-axis denotes the smoothed EVI values. The red line denotes the smoothed EVI values. The number in each panel denotes the extracted peak EVI days.

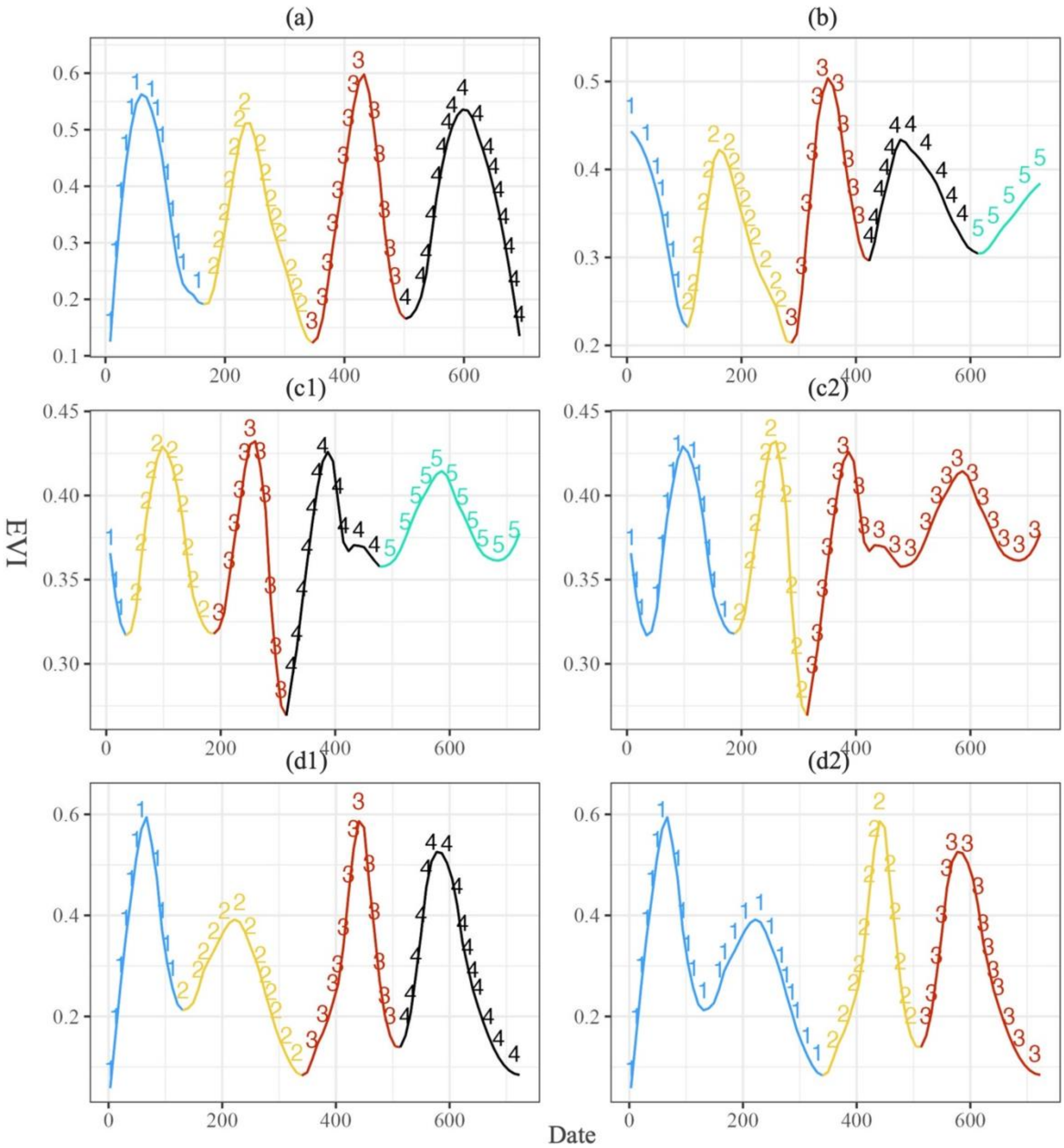


**Figure S3.** Example of the number of rice cropping season detection using Weibull function implemented via the "cardidates" package in R, and comparison of the parameters for detection. X-axis denotes the days from 1 January 2019 to 31 December 2020, and Y-axis denotes the smoothed EVI values. The peakwindow function was used to identify the number of peaks from smoothed EVI time series (e.g., Philippines (16.25°N, 121.75E°)) **(a)**, even though there is an incomplete downward-opening shape (e.g., Philippines (7.25°N, 124.25E°)) **(b)**. Comparison of the *mincut* setting on number of rice cropping season detection (e.g., Philippines (7.25°N, 124.25E°), the number of rice cropping seasons was 5 when *mincut* equals 0.9 **(c1)**, whereas the number of rice cropping seasons was 3 when *mincut* equals 0.8 **(c2)**. Similarly, comparison of the *minpeak* setting on the number of rice cropping seasons detection (e.g., Philippines (8.25°N, 122.25E°)), the number of rice cropping seasons was 4 when *minpeak* equals 0.6 **(d1)**, whereas the number of rice cropping seasons was 3 when *minpeak* equals 0.7 **(d2)**.

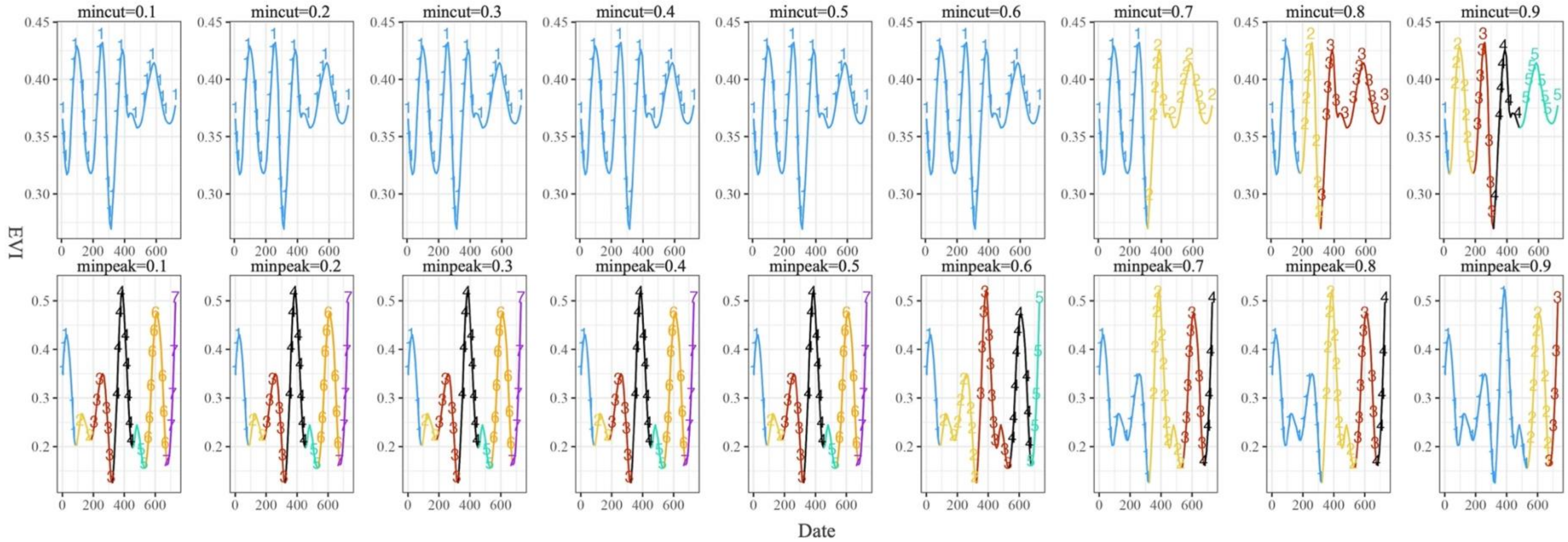


**Figure S4.** Comparison in *mincut* and *minpeak* values in peakwindow function of “cardidate” R package. The *mincut* and *minpeak* values are 0.1, 0.2, 0.3, 0.4, 0.5, 0.6, 0.7, 0.8, and 0.9. The two grids are located at 7.25°N, 124.25E° and 15.75°N, 119.75E° in the Philippines.

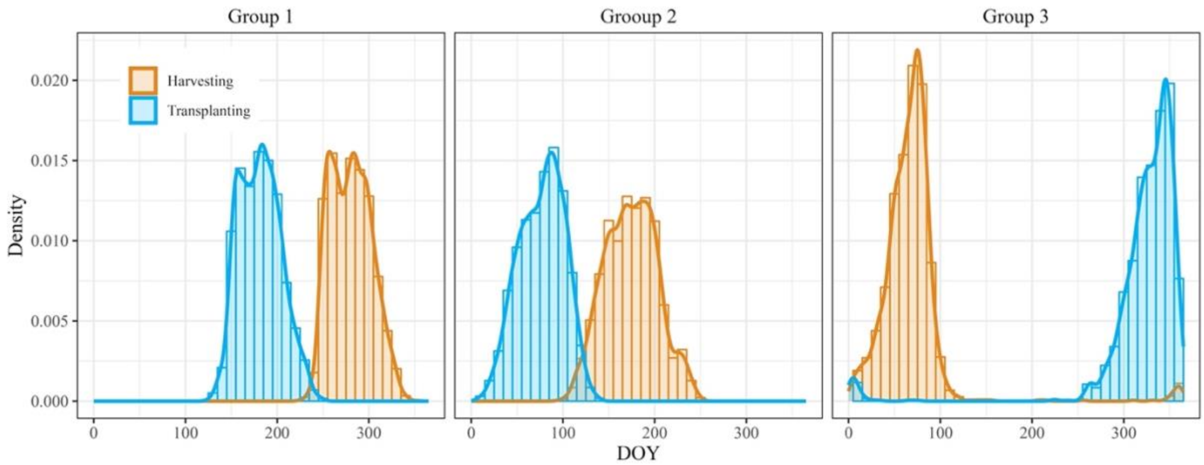


**Figure S5.** Distribution of transplanting and harvesting dates for three groups. Blue and orange represent the transplanting date and the harvesting date, respectively.

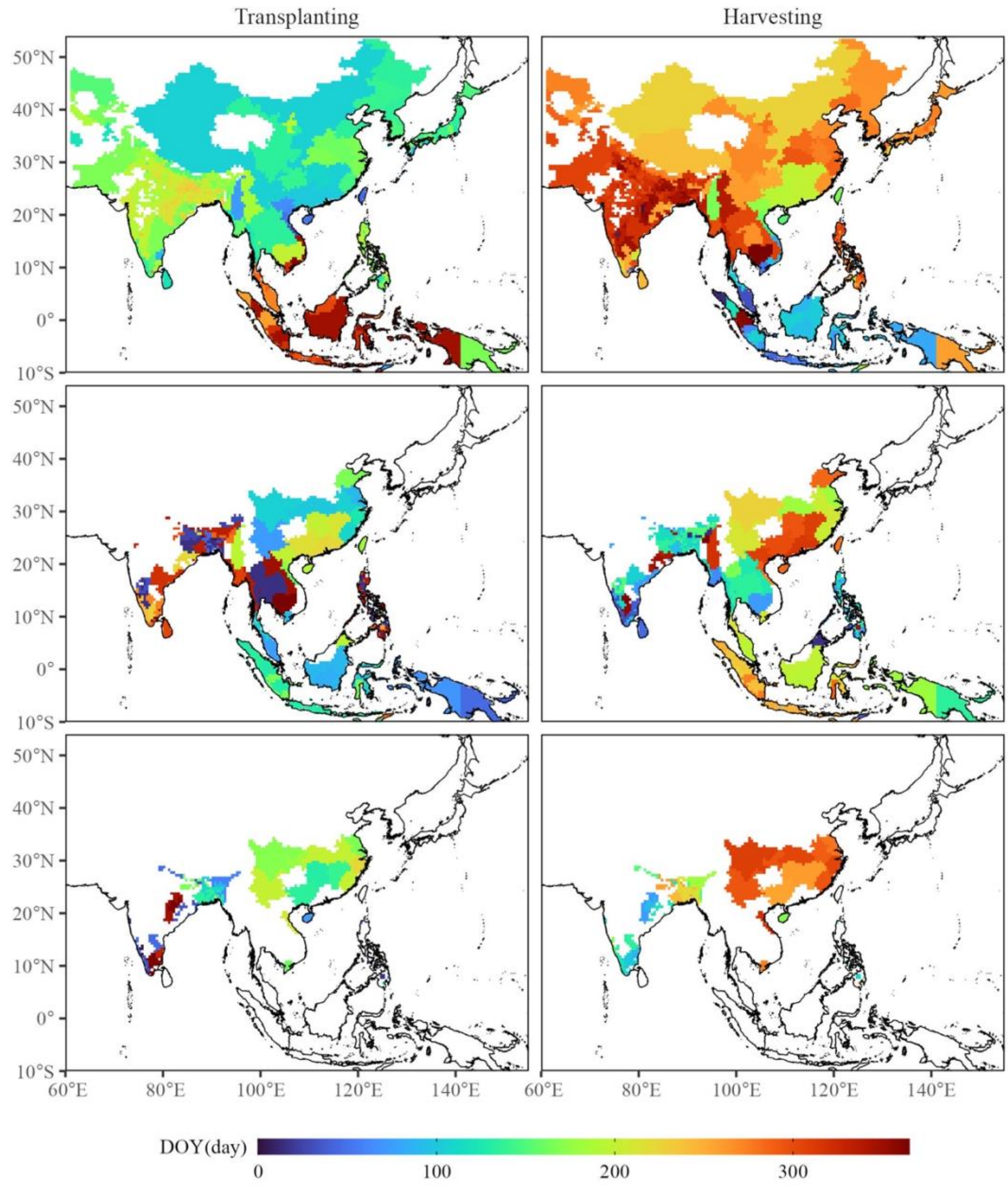


**Figure S6.** Transplanting and harvesting dates from the RiceAtlas. The gradient from blue to red in the legend denotes the respective transplanting and harvesting dates.

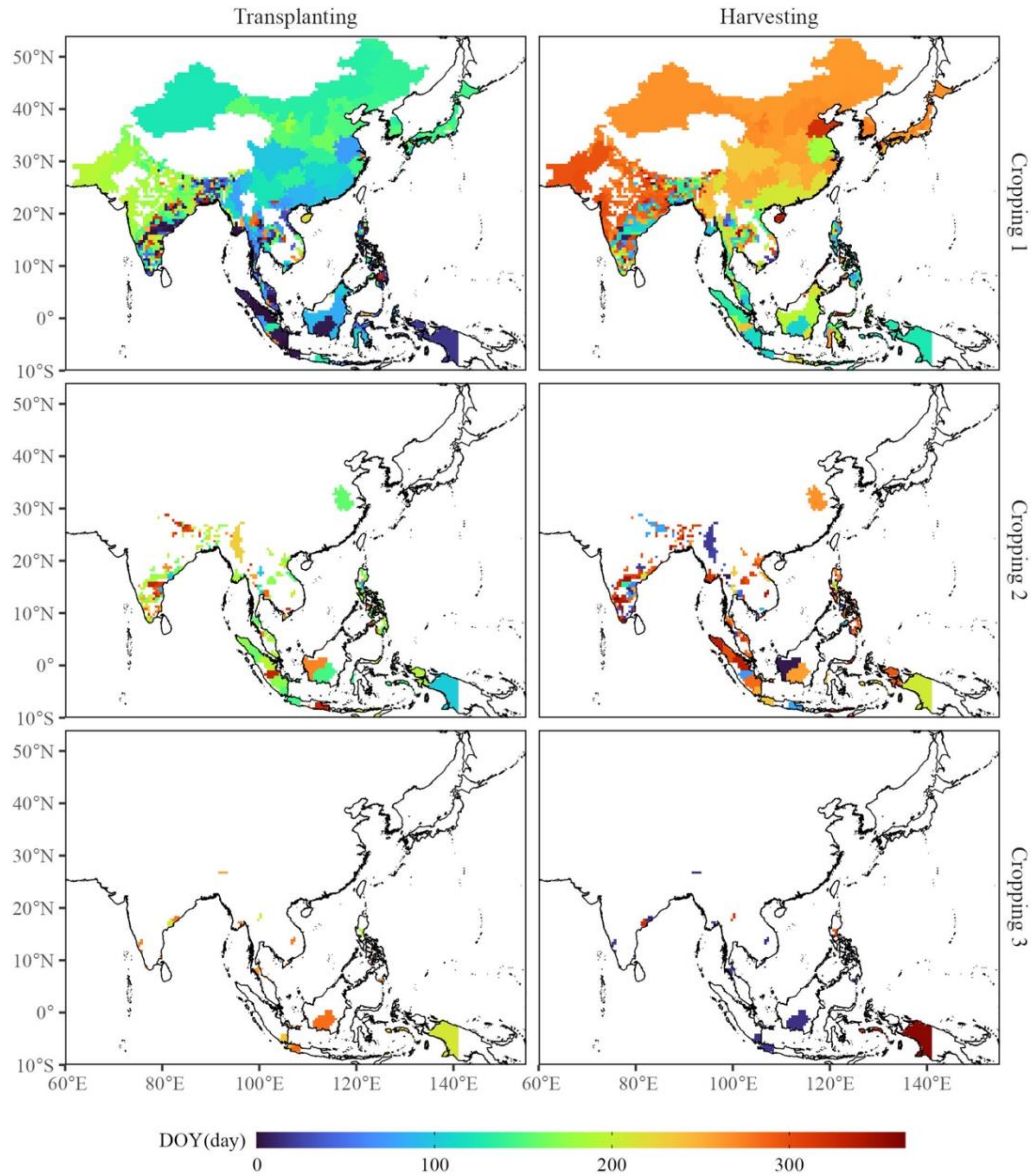


**Figure S7.** Transplanting and harvesting dates from the RICA. The gradient from blue to red in the legend denotes the respective transplanting and harvesting dates.

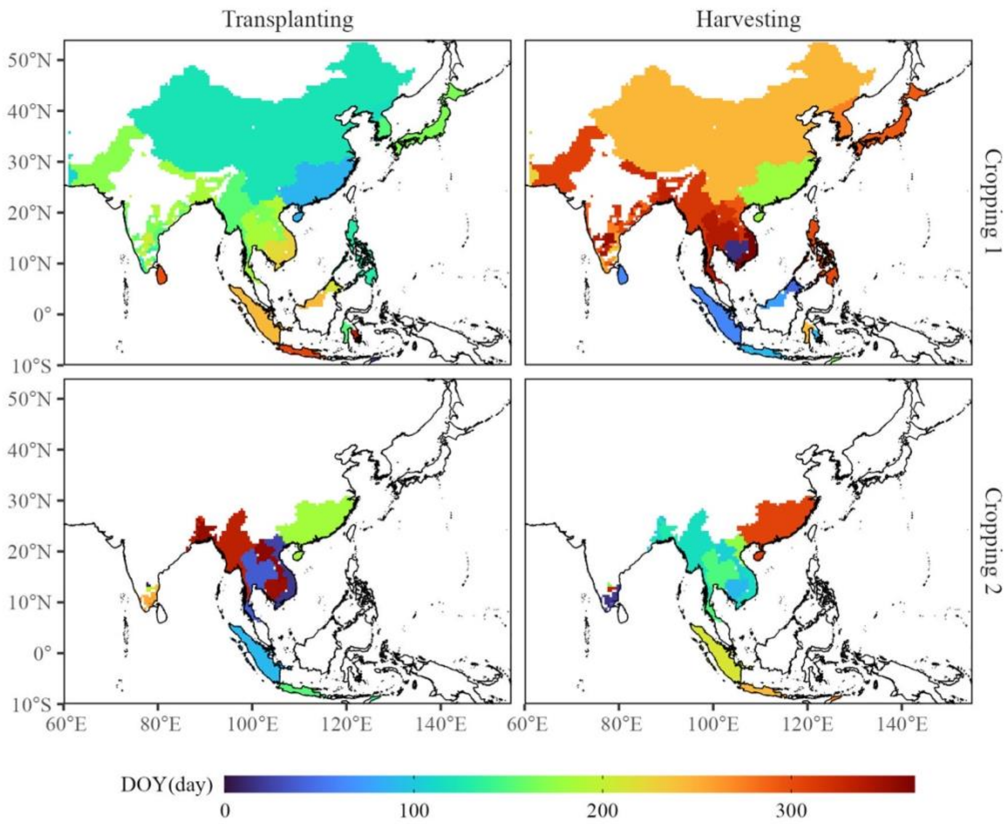


**Figure S8.** Transplanting and harvesting dates from the SAGE. The gradient from blue to red in the legend denotes the respective transplanting and harvesting dates.

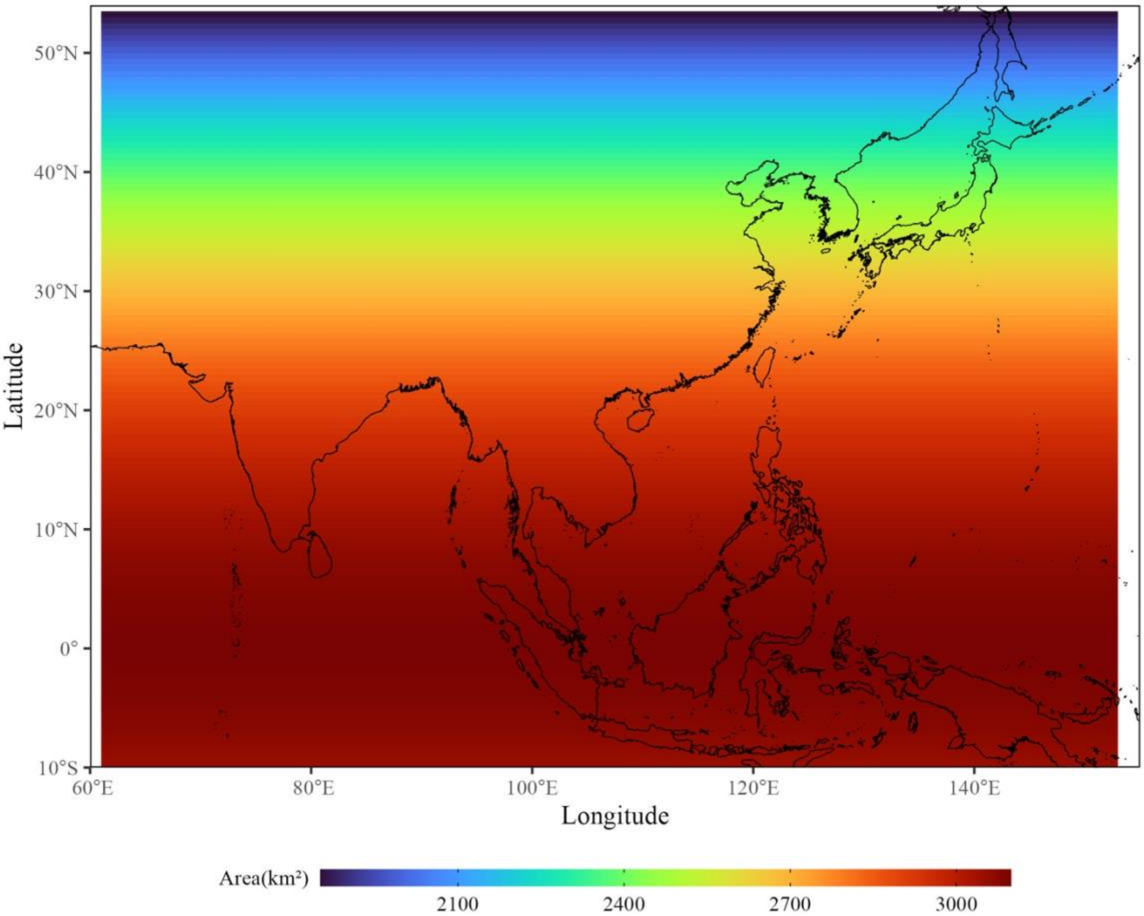


**Figure S9.** Area of each grid cell (0.5°) on the ellipsoidal earth within the study area (10° S to 53.5° N, 61° E to 153° E).

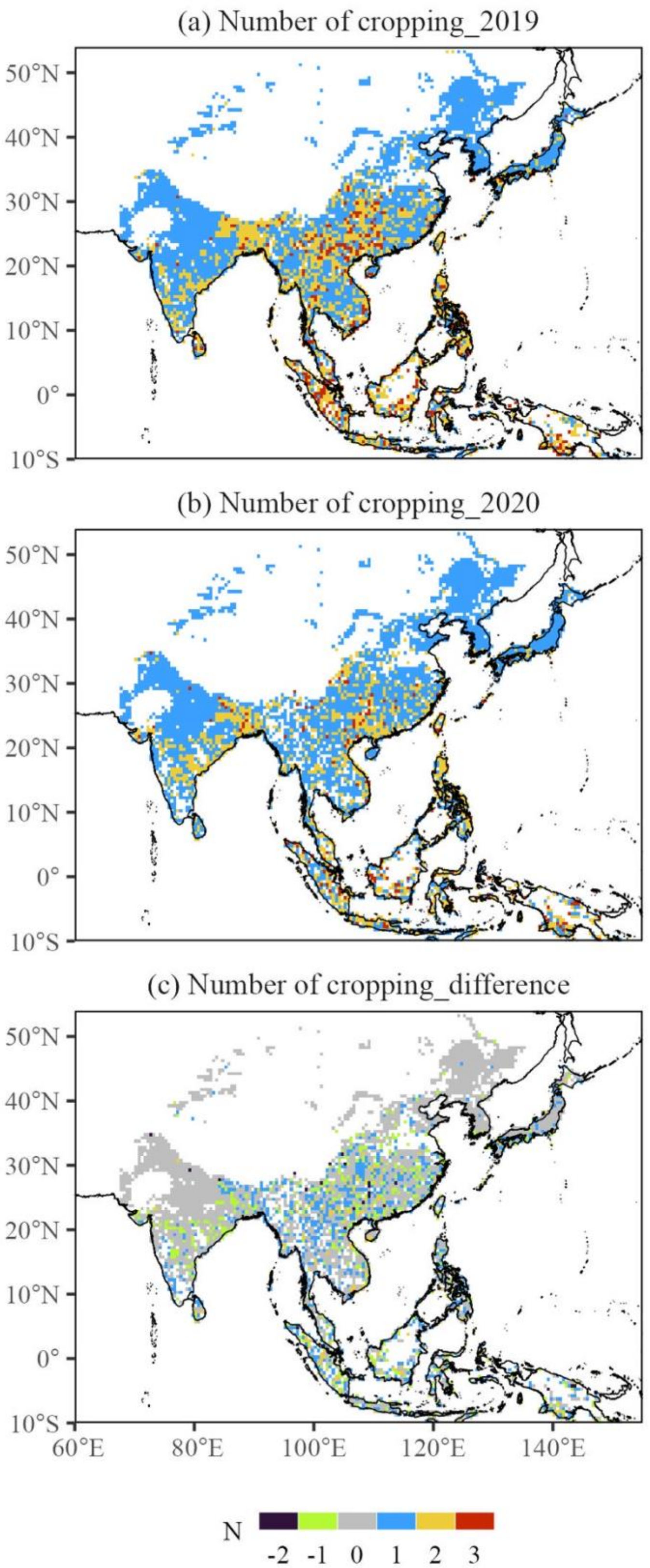


**Figure S10.** Detected number of rice cropping seasons in 2019 **(a)** and 2020 **(b)**, and difference in number of rice cropping seasons during the two years **(c)**.

**S1. Performance of the proposed rice calendar**

The performance of the proposed rice calendar in determining the transplanting and harvesting dates was assessed using the coefficient of determination ($R^2$), bias error (Bias), Mean Absolute Error (MAE), and Root Mean Square Error (RMSE) which were calculated as follows:

$$R^2 = 1\text{-}\frac{(\sum_{i=1}^{n}(y_i-\bar{y})(s_i-\bar{s}))^2}{\sum_{i=1}^{n}(y_i-\bar{y})^2-\sum_{i=1}^{n}(s_i-\bar{s})^2} \quad (1)$$

$$\text{Bias} = \frac{1}{n}\sum_{i=1}^{n}(y_i - s_i) \quad (2)$$

$$\text{MAE} = \frac{1}{n}\sum_{i=1}^{n}|y_i - s_i| \quad (3)$$

$$\text{RMSE} = \sqrt{\frac{1}{n}\sum_{i=1}^{n}(y_i - s_i)^2} \quad (4)$$

where $y_i$ and $\bar{y}$ are the phenological dates from the proposed rice calendar for sample grid ($i$) and the corresponding mean value, respectively, $s_i$ and $\bar{s}$ are the phenological dates from the reference rice calendar for sample grid ($i$) and the corresponding mean value, respectively, and $n$ represents the number of sampled phenological dates.

**S2. Optimal time window for transplanting and harvesting dates detection**

To identify the optimal time window for detection of the transplanting and harvesting dates, the time window for detection of the minimum VH was set from 120 days before the date of peak EVI to 45 days before the date of peak EVI ($DOY_{EVI_{max}}$), or from the first day of EVI arc ($DOY_{EVI\ arc_{first\ day}}$) to 45 days before the date of peak EVI. The time window for detection of the peak NDYI was set from 13 days after the peak EVI date to 55 days after the date of peak EVI, or from 13 days after the peak EVI date to the last day of the EVI arc ($DOY_{EVI\ arc_{last\ day}}$). It can be shown as follow table.

**Table S1.** Optimal time window for transplanting and harvesting dates detection

| Time window | Transplanting date | Harvesting date |
|---|---|---|
| 1 | $[DOY_{EVI_{max}} - 120, \quad DOY_{EVI_{max}} - 45]$ | $[DOY_{EVI_{max}} + 13, \quad DOY_{EVI_{max}} + 55]$ |
| 2 | $[DOY_{EVI\ arc_{first\ day}}, \quad DOY_{EVI_{max}} - 45]$ | $[DOY_{EVI_{max}} + 13, \quad DOY_{EVI\ arc_{last\ ay}}]$ |

**S3. Site validation**

To further validate the proposed rice calendar, site phenological dates close to the experimental period were collected from two sources: 1) 39 sites recorded in the literatures, and 2) observations from one site in the PhenoCam dataset. The transplanting and harvesting dates were directly extracted from the literature records for the 39 sites. Since there is only one rice paddy site located in monsoon Asia in the PhenoCam dataset, the Jurong site provides a time series of vegetation phenological observations derived from conventional visible-wavelength automated digital camera imagery. The transplanting and harvesting dates for all 40 sites are summarized in Table S2. These 40 sites are representative due to their wide coverage across monsoon Asia (Fig. S11).

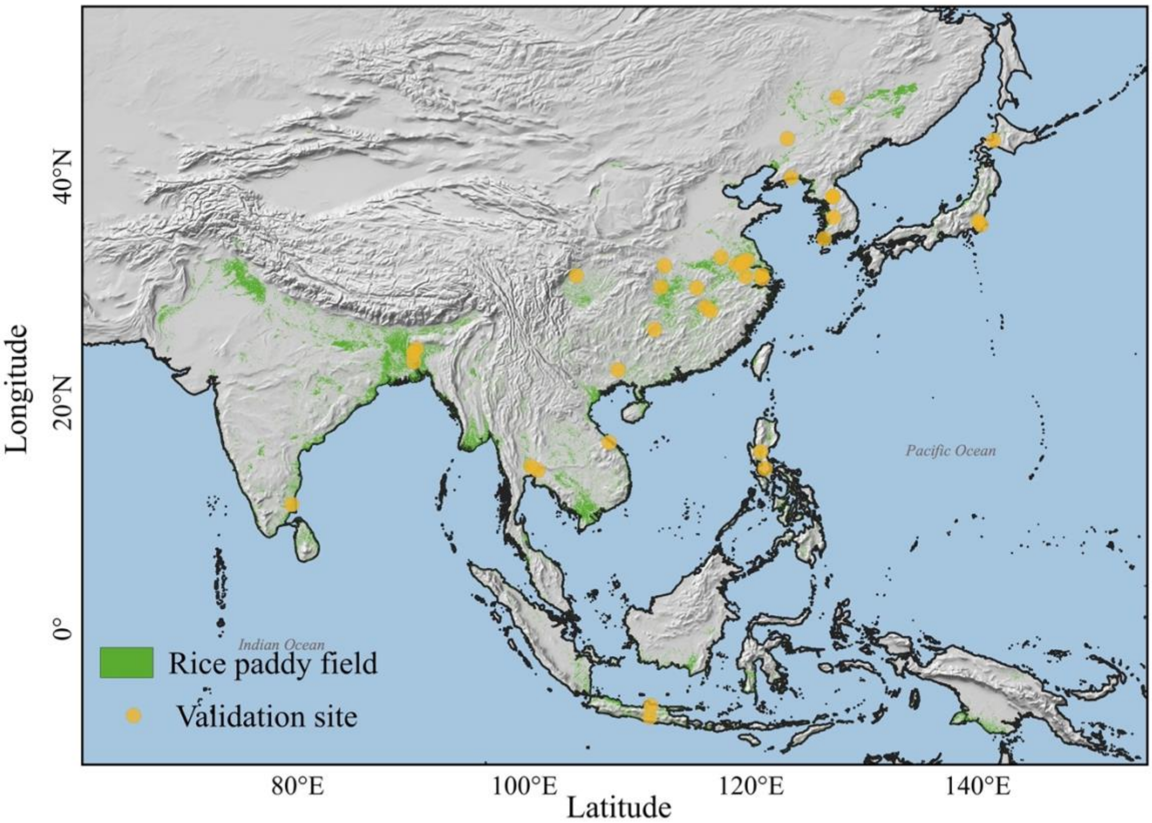


**Figure S11.** Location of the validation sites in monsoon Asia. Green areas indicate rice paddy fields. Yellow circles denote the validation site collected from the literatures and dataset.

**Table S2.** Transplanting date and harvesting date for 40 sites, along with the corresponding phenological dates from rice calendars at each site location

| **Country** | **Latitude** | **Longitude** | **T_ site** | **H_ site** | **T_ MARC** | **H_ MARC** | **T_ RiceAtlas** | **H_ RiceAtlas** | **T_ RICA** | **H_ RICA** | **T_ SAGE** | **H_ SAGE** | **Reference** |
|---|---|---|---|---|---|---|---|---|---|---|---|---|---|
| Thailand | 14.01 °N | 101.22 °E | 182 | 273 | 190.34 | 285.34 | 135 | 306 | 138.73 | 264.66 | 185.5 | 339 | Chidthaisong et al., 2018 |
| South Korea | 36.37 °N | 127.33 °E | 149 | 289 | 164.25 | 266.18 | 148 | 275 | 145.08 | 277.41 | 151 | 274 | Choi et al., 2019 |
| China | 30.97 °N | 121.01 °E | 175 | 297 | 175.61 | 269.95 | 160 | 304 | 262.18 | 19.18 | 121.5 | 245.5 | Fang et al., 2021 |
| Japan | 35.71 °N | 140.34 °E | 158 | 266 | 157.68 | 251.79 | 117 | 244 | 124.19 | 252.35 | 167 | 291 | Fawibe et al., 2019 |
| China | 32.10 °N | 112.40 °E | 152 | 274 | 159.85 | 253.46 | 166 | 294 | 136.64 | 257.02 | 121.5 | 245.5 | Feng et al., 2021 |
| Bangladesh | 24.75 °N | 90.50 °E | 20 | 119 | 34.10 | 128.45 | 5 | 110 | 17.83 | 129.72 | -12 | 127.5 | Forhad et al., 2019 |
| China | 30.21 °N | 112.09 °E | 157 | 257 | 150.93 | 250.49 | 166 | 294 | 136.64 | 257.02 | 121.4 | 245.5 | Fu et al., 2019 |
| South Korea | 38.20 °N | 127.25 °E | 121 | 246 | 155.95 | 260.51 | 140 | 267 | 128.19 | 265.18 | 151 | 274 | Huang et al., 2018 |
| South Korea | 38.20 °N | 127.25 °E | 129 | 257 | 155.95 | 260.51 | 140 | 267 | 128.19 | 265.18 | 151 | 274 | Hwang et al., 2020 |
| Philippines | 14.16 °N | 121.26 °E | 30 | 133 | -28.93 | 68.77 | −16 | 105 | -8.76 | 105.02 | 130 | 301 | Islam et al., 2020 |
| Bangladesh | 23.60 °N | 90.25 °E | 25 | 120 | 52.86 | 152.85 | 10 | 105 | 173.01 | 285.63 | -12 | 127.5 | Islam et al., 2020 |
| Bangladesh | 24.44 °N | 90.24 °E | 23 | 118 | 37.16 | 134.05 | 15 | 120 | 50.36 | 154.87 | -12 | 127.5 | Islam et al., 2020 |

| | | | | | | | | | | | | | |
|---|---|---|---|---|---|---|---|---|---|---|---|---|---|
| South Korea | 38.20 ºN | 127.25 ºE | 135 | 257 | 155.95 | 260.51 | 140 | 267 | 128.19 | 265.18 | 151 | 274 | Jeong et al., 2020 |
| South Korea | 34.48 ºN | 126.48 ºE | 152 | 306 | 167.17 | 265.46 | - | - | - | - | 151 | 274 | Jeong et al., 2020 |
| China | 22.88 ºN | 108.29 ºE | 102 | 199 | 86.25 | 172.03 | 101 | 195 | 88.08 | 210.59 | 88 | 179.5 | Li et al., 2020 |
| China | 30.14 ºN | 115.25 ºE | 121 | 229 | 161.46 | 252.94 | 100 | 181 | 136.64 | 257.02 | 121.5 | 245.5 | Liang et al., 2019 |
| China | 28.44 ºN | 116.00 ºE | 195 | 304 | 186.04 | 287.20 | 140 | 260 | 109.38 | 252.92 | 182.5 | 306 | Liu et al., 2019a |
| China | 28.10 ºN | 116.50 ºE | 116 | 203 | 104.35 | 195.59 | 105 | 201 | 109.38 | 252.92 | 88 | 179.5 | Liu et al., 2019b |
| China | 31.22 ºN | 104.62 ºE | 149 | 268 | 175.62 | 269.52 | 135 | 270 | 99.7 | 235.3 | 121.5 | 245.5 | Liu et al., 2021 |
| Thailand | 14.37 ºN | 100.61 ºE | 305 | 57 | 309.77 | 43.72 | 390 | 135 | 338.71 | 103.1 | 37.5 | 148.5 | Maneepitak et al., 2019 |
| Japan | 43.18 ºN | 141.44 ºE | 144 | 258 | 175.09 | 268.64 | - | - | - | - | 167 | 291 | Naser et al., 2020 |
| China | 46.95 ºN | 127.67 ºE | 139 | 264 | 155.51 | 256.52 | 135 | 266 | 137.53 | 261.92 | 121.5 | 245.5 | Nie et al., 2020 |
| Indonesia | -7.79 ºN | 111.10 ºE | 102 | 203 | 69.22 | 160.35 | 130 | 248 | - | - | 151 | 243 | Nugroho et al., 2018 |
| Japan | 36.03 ºN | 140.11 ºE | 140 | 271 | 150.23 | 257.62 | 126 | 251 | 132.97 | 256.28 | 167 | 291 | Okamura et al., 2018 |
| India | 11.00 ºN | 79.50 ºE | 167 | 264 | 194.62 | 310.46 | 181 | 301 | 199.21 | 315.07 | 133.5 | 231.5 | Oo et al., 2020 |
| China | 26.45 ºN | 111.52 ºE | 116 | 199 | 111.23 | 198.67 | 110 | 200 | 109.94 | 240.2 | 88 | 179.5 | Raheem et al., 2019 |
| Indonesia | -6.78 ºN | 111.20 ºE | 92 | 196 | 93.48 | 183.12 | 130 | 248 | - | - | 151 | 243 | Setyanto et al., 2018 |

| | | | | | | | | | | | | | |
|---|---|---|---|---|---|---|---|---|---|---|---|---|---|
| Philippines | 15.67 ºN | 120.90 ºE | 168 | 260 | 187.61 | 289.05 | 189 | 285 | 192.15 | 294.22 | 130 | 301.5 | Sibayan et al., 2018 |
| China | 31.16 ºN | 119.54 ºE | 160 | 313 | 171.34 | 267.08 | 166 | 280 | 75.83 | 186.61 | 121.5 | 245.5 | Sun et al., 2019a |
| China | 39.88 ºN | 123.58 ºE | 149 | 262 | 159.20 | 264.02 | 140 | 284 | 141.37 | 264.41 | 121.5 | 245.5 | Sun et al., 2019b |
| Vietnam | 16.47 ºN | 107.52 ºE | 20 | 140 | 52.27 | 143.62 | 30 | 140 | 7.2 | 134.67 | 18 | 113.5 | Tran et al., 2018 |
| Vietnam | 16.47 ºN | 107.52 ºE | 162 | 252 | 150.62 | 247.52 | 155 | 265 | 147.96 | 242.73 | 227 | 365 | Tran et al., 2018 |
| China | 32.86 ºN | 117.40 ºE | 180 | 301 | 173.67 | 271.41 | 161 | 274 | 155.72 | 265.26 | 121.5 | 245.5 | Wang et al., 2020 |
| China | 32.21 ºN | 118.71 ºE | 170 | 299 | 176.84 | 271.19 | 166 | 280 | 75.83 | 186.61 | 121.5 | 245.5 | Wang et al., 2021 |
| China | 43.32 ºN | 123.23 ºE | 149 | 289 | 155.60 | 253.35 | 105 | 227 | 131.48 | 261.93 | 121.5 | 245.5 | Wu et al., 2019 |
| China | 31.25 ºN | 120.96 ºE | 181 | 304 | 175.61 | 269.95 | 166 | 280 | 75.83 | 186.61 | 121.5 | 245.5 | Yang et al., 2018 |
| China | 32.58 ºN | 119.70 ºE | 173 | 307 | 181.15 | 277.72 | 166 | 280 | 75.83 | 186.61 | 121.5 | 245.5 | Yuan et al., 2021 |
| China | 32.50 ºN | 119.42 ºE | 164 | 292 | 182.86 | 279.63 | 166 | 280 | 75.83 | 186.61 | 121.5 | 245.5 | Zhang et al., 2018 |
| China | 32.30 ºN | 119.25 ºE | 164 | 294 | 179.19 | 277.27 | 166 | 280 | 75.83 | 186.61 | 121.5 | 245.5 | Zhang et al., 2019 |
| China (Jurong, PhenoCam site) | 119.22 ºN | 31.81 ºE | - | 273.6 | 177.84 | 274.33 | - | 280 | 75.83 | 186.61 | 121.5 | 245.5 | Seyednasrollah et al., 2019 |

Note: T_site and H_site denote the transplanting date and harvesting date of sites from literatures and dataset. T_MARC and H_MARC denote the transplanting date and harvesting date of the proposed rice calendar at each site location. T_RiceAtlas and H_RiceAtlas denote the transplanting date and harvesting date of the RiceAtlas rice calendar at each site location. T_RICA and H_RICA denote the transplanting date and harvesting date of the RICA rice calendar at each site location. T_SAGE and H_SAGE denote the transplanting date and harvesting date of the SAGE rice calendar at each site location. '-' denotes phenological dates are not available. Phenological dates less than 0 indicate that the day has been subtracted by 365 days for easy comparison

### S3.1 Comparison of transplanting and harvesting dates between proposed rice calendar and site records

The transplanting and harvesting dates from the proposed rice calendar were further compared with those from the site records. The transplanting and harvesting dates were firstly extracted from the proposed rice calendar at each site location as shown in Table S2. The transplanting dates of the proposed rice calendar are consistent with those site records, with $R^2$ of 0.90, Bias of 7.99 days, MAE of 16.32 days, and RMSE of 19.00 days (Fig. S12). Additionally, the harvesting dates of the proposed rice calendar are correlated with those of the site records with $R^2$ of 0.87, Bias of −9.07 days, MAE of 19.58 days, and RMSE of 22.43 days (Fig. S12). This site validation demonstrates the efficacy of the proposed rice calendar.

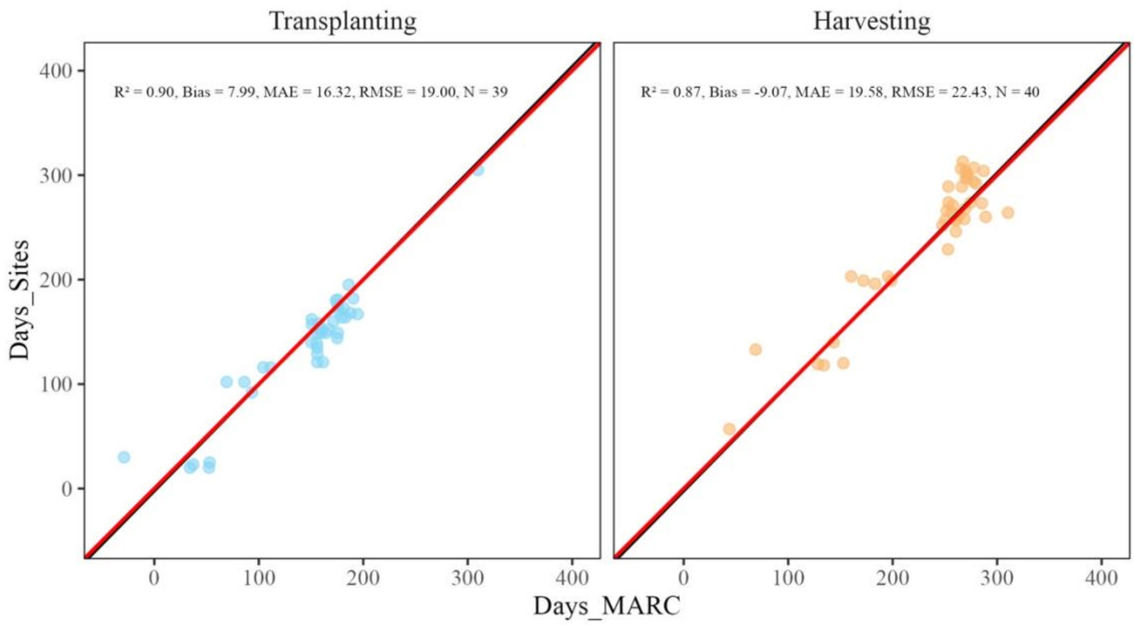


**Figure S12.** Comparison of transplanting date and harvesting date between the proposed rice calendar and site records. Blue and orange points represent the transplanting date and harvesting date, respectively. Red and black solid lines represent the 1:1 line and regression, respectively.

### S3.2 Comparison of transplanting and harvesting dates between other rice calendars and site records

To evaluate the superiority of the proposed rice calendar, the transplanting and harvesting dates from other rice calendars were compared with those from the site records. The transplanting and harvesting dates from RiceAtlas, RICA, and SAGE rice calendars were extracted at each site location, as shown in Table S2. The transplanting dates of RiceAtlas, RICA, and SAGE rice calendars were correlated with the site records, with $R^2$ of 0.86, Bias of −2.41 days, MAE of 19.10 days, and RMSE of 26.56 days; $R^2$ of 0.42, Bias of −20.85 days, MAE of 41.41 days, and RMSE of 57.66 days; $R^2$ of 0.64, Bias of −11.28 days, MAE of 37.08 days, and RMSE of 45.31 days, respectively (Fig. S13). Similarly, the harvesting dates of RiceAtlas, RICA, and SAGE rice calendars were correlated with the site records, with $R^2$ of 0.80, Bias of 2.96 days, MAE of 22.75 days, and RMSE of 29.51 days; $R^2$ of 0.11, Bias of −29.29 days, MAE of 56.25 days, and RMSE of 85.61 days; $R^2$ of 0.44, Bias of −6.88 days, MAE of 43.60 days, and RMSE of 61.10 days, respectively (Fig. S13). The phenological dates of the proposed rice calendar were found to be closer to the site records compared to those of three rice calendars. The good performance in the site validation clearly demonstrates the ability and advantage of the proposed rice calendar in retrieving rice transplanting and harvesting dates.

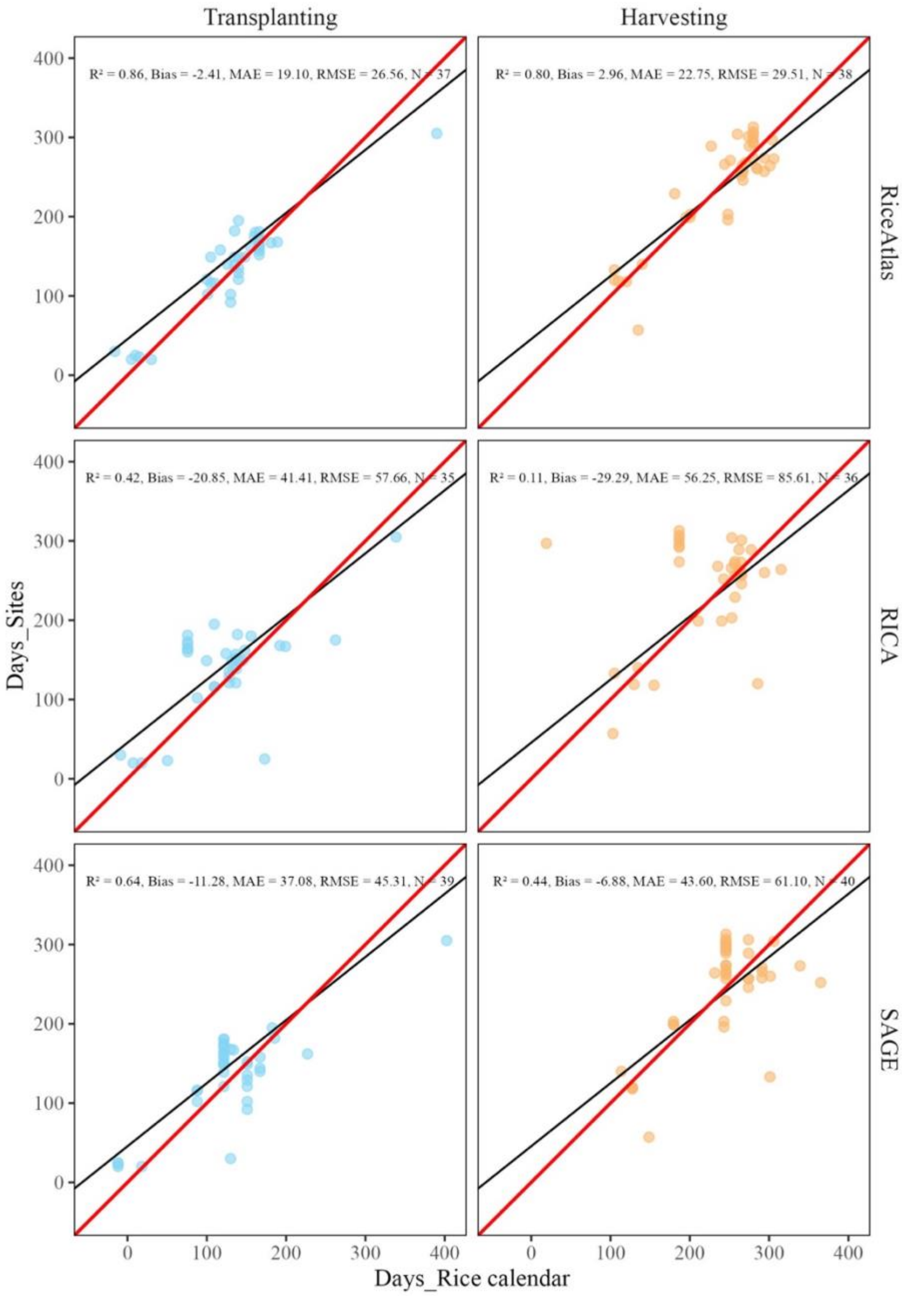


**Figure S13.** Comparison of transplanting date and harvesting date between the rice calendars (RiceAtlas, RICA, and SAGE) and site records. Blue and orange points represent the transplanting date and harvesting date, respectively. Red and black solid lines represent the 1:1 line and regression, respectively.

**References**


Chidthaisong, A., Cha-un, N., Rossopa, B., Buddaboon, C., Kunuthai, C., Sriphirom, P., Towprayoon, S., Tokida, T., Padre, A. T., and Minamikawa, K.: Evaluating the effects of alternate wetting and drying (AWD) on methane and nitrous oxide emissions from a paddy field in Thailand, Soil Sc. Plant Nutr., 64, 31–38, https://doi.org/10.1080/00380768.2017.1399044, 2018.

Choi, E. J., Jeong, H. C., Kim, G. Y., Lee, S. I., Gwon, H. S., Lee, J. S., and Oh, T. K.: Assessment of methane emission with application of rice straw in a paddy field. Korean J. Agric. Sci., 46(4), 857–868. https://doi.org/10.7744/KJOAS.20190069, 2019.

Fang, K., Gao, H., Sha, Z., Dai, W., Yi, X., Chen, H., and Cao, L.: Mitigating global warming potential with increase net ecosystem economic budget by integrated rice-frog farming in eastern China, Agric. Ecosyst. Environ., 308, 107235, https://doi.org/10.1016/j.agee.2020.107235, 2021.

Fawibe, O. O., Honda, K., Taguchi, Y., Park, S., and Isoda, A.: Greenhouse gas emissions from rice field cultivation with drip irrigation and plastic film mulch, Nutr. Cycl. Agroecosyst., 113, 51–62, https://doi.org/10.1007/s10705-018-9961-3, 2019.

Feng, Z. Y., Qin, T., Du, X. Z., Sheng, F., and Li, C. F.: Effects of irrigation regime and rice variety on greenhouse gas emissions and grain yields from paddy fields in central China, Agric. Water Manage., 250, 106830, https://doi.org/10.1016/j.agwat.2021.106830, 2021.

Forhad, A. B. M., Ahatun, R., and Islam, M. Z.: Soil microbial status and methane emission under waste materials application in rice paddy field. International Journal of Environmental Sciences & Natural Resources, 18(1), 555977, https://doi.org/10.19080/IJESNR.2019.18.555977, 2019.

Fu, J., Wu, Y., Wang, Q., Hu, K., Wang, S., Zhou, M., Hayashi, K., Wang, H., Zhan, X., Jian, Y., Cai, C., Song, M., Liu, K., Wang, Y., Zhou, F., and Zhu, J.: Importance of subsurface fluxes of water, nitrogen and phosphorus from rice paddy fields relative to surface runoff, Agric. Water Manage., 213, 627–635, https://doi.org/10.1016/j.agwat.2018.11.005, 2019.

Huang, Y., Ryu, Y., Jiang, C., Kimm, H., Kim, S., Kang, M., and Shim, K.: BESS-Rice: A remote sensing derived and biophysical process-based rice productivity simulation model, Agric. For. Meteorol., 256–257, 253–269, https://doi.org/10.1016/j.agrformet.2018.03.014, 2018.

Hwang, Y., Ryu, Y., Huang, Y., Kim, J., Iwata, H., and Kang, M.: Comprehensive assessments of carbon dynamics in an intermittently-irrigated rice paddy, Agricu. For. Meteorol., 285–286, 107933, https://doi.org/10.1016/j.agrformet.2020.107933, 2020.

Islam, S. F.-u., de Neergaard, A., Sander, B. O., Jensen, L. S., Wassmann, R., and van Groenigen, J. W.: Reducing greenhouse gas emissions and grain arsenic and lead levels without compromising yield in organically produced rice, Agricu. Ecosyst. Environ., 295, 106922, https://doi.org/10.1016/j.agee.2020.106922, 2020.

Jeong, S., Ko, J., Kang, M., Yeom, J., Ng, C. T., Lee, S.H., Lee, Y. G., and Kim, H. Y.: Geographical variations in gross primary production and evapotranspiration of paddy rice in the Korean Peninsula, Sci. Total Environ., 714, 136632, https://doi.org/10.1016/j.scitotenv.2020.136632, 2020.

Li, L., Li, F., and Dong, Y.: Greenhouse Gas Emissions and Global Warming Potential in Double-Cropping Rice Fields as Influenced by Two Water-Saving Irrigation Modes in South China, J. Soil Sci. Plant Nutr., 20, 2617–2630, https://doi.org/10.1007/s42729-020-00328-5, 2020.

Ling, X., Zhang, T., Deng, N., Yuan, S., Yuan, G., He, W., Cui, K., Nie, L., Peng, S., Li, T., and Huang, J.: Modelling rice growth and grain yield in rice ratooning production system, Field Crop. Res., 241, 107574, https://doi.org/10.1016/j.fcr.2019.107574, 2019.

Liu, B., Cui, Y., Luo, Y., Shi, Y., Liu, M., and Liu, F.: Energy partitioning and evapotranspiration over a rotated paddy field in Southern China, Agric. For. Meteorol., 276–277, 107626,

https://doi.org/10.1016/j.agrformet.2019.107626, 2019a.
Liu, J., Huang, X., Jiang, H., and Chen, H.: Sustaining yield and mitigating methane emissions from rice production with plastic film mulching technique, Agric. Water Manage., 245, 106667, https://doi.org/10.1016/j.agwat.2020.106667, 2021.
Liu, Y., Tang, H., Muhammad, A., Zhong, C., Li, P., Zhang, P., Yang, B., and Huang, G.: Rice Yield and Greenhouse Gas Emissions Affected by Chinese Milk Vetch and Rice Straw Retention with Reduced Nitrogen Fertilization, Agrono. J., 111, 3028–3038, https://doi.org/10.2134/agronj2019.03.0145, 2019b.
Maneepitak, S., Ullah, H., Datta, A., Shrestha, R. P., Shrestha, S., and Kachenchart, B.: Effects of water and rice straw management practices on water savings and greenhouse gas emissions from a double-rice paddy field in the Central Plain of Thailand, Eur. J. Agron., 107, 18–29, https://doi.org/10.1016/j.eja.2019.04.002, 2019.
Naser, H. M., Nagata, O., Sultana, S., and Hatano, R.: Carbon Sequestration and Contribution of $CO_2$, $CH_4$ and $N_2O$ Fluxes to Global Warming Potential from Paddy-Fallow Fields on Mineral Soil Beneath Peat in Central Hokkaido, Japan, Agriculture, https://doi.org/10.3390/agriculture10010006, 2020.
Nie, T., Chen, P., Zhang, Z., Qi, Z., Zhao, J., Jiang, L., and Lin, Y.: Effects of irrigation method and rice straw incorporation on $CH_4$ emissions of paddy fields in Northeast China, Paddy Water Environ., 18, 111-120, https://doi.org/10.1007/s10333-019-00768-5, 2020.
Nugroho, B. D. A., Toriyama, K., Kobayashi, K., Arif, C., Yokoyama, S., and Mizoguchi, M.: Effect of intermittent irrigation following the system of rice intensification (SRI) on rice yield in a farmer's paddy fields in Indonesia, Paddy Water Environ., 16, 715–723, https://doi.org/10.1007/s10333-018-0663-x, 2018.
Okamura, M., Arai-Sanoh, Y., Yoshida, H., Mukouyama, T., Adachi, S., Yabe, S., Nakagawa, H., Tsutsumi, K., Taniguchi, Y., Kobayashi, N., and Kondo, M.: Characterization of high-yielding rice cultivars with different grain-filling properties to clarify limiting factors for improving grain yield, Field Crop. Res., 219, 139–147, https://doi.org/10.1016/j.fcr.2018.01.035, 2018.
Oo, A. Z., Sudo, S., Fumoto, T., Inubushi, K., Ono, K., Yamamoto, A., Bellingrath-Kimura, S. D., Win, K. T., Umamageswari, C., Bama, K. S., Raju, M., Vanitha, K., Elayakumar, P., Ravi, V., and Ambethgar, V.: Field Validation of the DNDC-Rice Model for Methane and Nitrous Oxide Emissions from Double-Cropping Paddy Rice under Different Irrigation Practices in Tamil Nadu, India, Agriculture, https://doi.org/10.3390/agriculture10080355, 2020.
Raheem, A., Zhang, J., Huang, J., Jiang, Y., Siddik, M. A., Deng, A., Gao, J., and Zhang, W.: Greenhouse gas emissions from a rice-rice-green manure cropping system in South China, Geoderma, 353, 331–339, https://doi.org/10.1016/j.geoderma.2019.07.007, 2019.
Setyanto, P., Pramono, A., Adriany, T. A., Susilawati, H. L., Tokida, T., Padre, A. T., and Minamikawa, K.: Alternate wetting and drying reduces methane emission from a rice paddy in Central Java, Indonesia without yield loss, Soil Sci. Plant Nutr., 64, 23–30, https://doi.org/10.1080/00380768.2017.1409600, 2018.
Seyednasrollah, B., Young, A. M., Hufkens, K., Milliman, T., Friedl, M. A., Frolking, S., Richardson, A. D., Abraha, M., Allen, D. W., Apple, M., Arain, M. A., Baker, J., Baker, J. M., Baldocchi, D., Bernacchi, C. J., Bhattacharjee, J., Blanken, P., Bosch, D. D., Boughton, R., Boughton, E. H., Brown, R. F., Browning, D. M., Brunsell, N., Burns, S. P., Cavagna, M., Chu, H., Clark, P. E., Conrad, B. J., Cremonese, E., Debinski, D., Desai, A. R., Diaz-Delgado, R., Duchesne, L., Dunn, A. L., Eissenstat, D. M., El-Madany, T., Ellum, D. S. S., Ernest, S. M., Esposito, A., Fenstermaker, L., Flanagan, L. B., Forsythe, B., Gallagher, J., Gianelle, D., Griffis, T., Groffman, P., Gu, L., Guillemot, J., Halpin, M., Hanson, P. J., Hemming, D., Hove, A. A., Humphreys, E. R., Jaimes-Hernandez, A., Jaradat, A. A., Johnson, J., Keel, E., Kelly, V. R., Kirchner, J. W., Kirchner, P. B., Knapp, M., Krassovski, M., Langvall, O., Lanthier, G., Maire, G. l., Magliulo, E., Martin, T. A., McNeil, B., Meyer, G. A., Migliavacca, M., Mohanty, B. P., Moore, C. E., Mudd, R., Munger, J. W., Murrell, Z. E., Nesic, Z., Neufeld,

H. S., O'Halloran, T. L., Oechel, W., Oishi, A. C., Oswald, W. W., Perkins, T. D., Reba, M. L., Rundquist, B., Runkle, B. R., Russell, E. S., Sadler, E. J., Saha, A., Saliendra, N. Z., Schmalbeck, L., Schwartz, M. D., Scott, R. L., Smith, E. M., Sonnentag, O., Stoy, P., Strachan, S., Suvocarev, K., Thom, J. E., Thomas, R. Q., Van den berg, A. K., Vargas, R., Verfaillie, J., Vogel, C. S., Walker, J. J., Webb, N., Wetzel, P., Weyers, S., Whipple, A. V., Whitham, T. G., Wohlfahrt, G., Wood, J. D., Wolf, S., Yang, J., Yang, X., Yenni, G., Zhang, Y., Zhang, Q., and Zona, D.: PhenoCam Dataset v2.0: Vegetation Phenology from Digital Camera Imagery, 2000–2018 [data set], ORNL Ridge, https://doi.org/10.3334/ORNLDAAC/1674, 2019.

Sibayan, E. B., Samoy-Pascual, K., Grospe, F. S., Casil, M. E. D., Tokida, T., Padre, A. T., and Minamikawa, K.: Effects of alternate wetting and drying technique on greenhouse gas emissions from irrigated rice paddy in Central Luzon, Philippines, Soil Sci. Plant Nutr., 64, 39–46, https://doi.org/10.1080/00380768.2017.1401906, 2018.

Sun, H., Lu, H., and Feng, Y.: Greenhouse gas emissions vary in response to different biochar amendments: an assessment based on two consecutive rice growth cycles, Environ. Sci. Pollut. Res., 26, 749–758, https://doi.org/10.1007/s11356-018-3636-0, 2019a.

Sun, Y., Xia, G., He, Z., Wu, Q., Zheng, J., Li, Y., Wang, Y., Chen, T., and Chi, D.: Zeolite amendment coupled with alternate wetting and drying to reduce nitrogen loss and enhance rice production, Field Crop. Res., 235, 95–103, https://doi.org/10.1016/j.fcr.2019.03.004, 2019b.

Tran, D. H., Hoang, T. N., Tokida, T., Tirol-Padre, A., and Minamikawa, K.: Impacts of alternate wetting and drying on greenhouse gas emission from paddy field in Central Vietnam, Soil Sci. Plant Nutr., 64, 14–22, https://doi.org/10.1080/00380768.2017.1409601, 2018.

Wang, H., Zhang, Y., Zhang, Y., McDaniel, M. D., Sun, L., Su, W., Fan, X., Liu, S., and Xiao, X.: Water-saving irrigation is a 'win-win' management strategy in rice paddies – With both reduced greenhouse gas emissions and enhanced water use efficiency, Agric. Water Manage., 228, 105889, https://doi.org/10.1016/j.agwat.2019.105889, 2020.

Wang, Y., Hu, Z., Shen, L., Liu, C., Islam, A. R. M. T., Wu, Z., Dang, H., and Chen, S.: The process of methanogenesis in paddy fields under different elevated $CO_2$ concentrations, Sci. Total Environ., 773, 145629, https://doi.org/10.1016/j.scitotenv.2021.145629, 2021.

Wu, K., Gong, P., Zhang, L., Wu, Z., Xie, X., Yang, H., Li, W., Song, Y., and Li, D.: Yield-scaled $N_2O$ and $CH_4$ emissions as affected by combined application of stabilized nitrogen fertilizer and pig manure in rice fields, Plant Soil Environ., 65, 497–502, https://doi.org/10.17221/286/2019-PSE, 2019.

Yang, S., Jiang, Z., Sun, X., Ding, J., and Xu, J.: Effects of Biochar Amendment on $CO_2$ Emissions from Paddy Fields under Water-Saving Irrigation, Int. J. Environ. Res. Public Health, https://doi.org/10.3390/ijerph15112580, 2018.

Yuan, M., Cai, C., Wang, X., Li, G., Wu, G., Wang, J., Geng, W., Liu, G., Zhu, J., and Sun, Y.: Warm air temperatures increase photosynthetic acclimation to elevated $CO_2$ concentrations in rice under field conditions, Field Crop. Res., 262, 108036, https://doi.org/10.1016/j.fcr.2020.108036, 2021.

Zhang, H., Yu, C., Kong, X., Hou, D., Gu, J., Liu, L., Wang, Z., and Yang, J.: Progressive integrative crop managements increase grain yield, nitrogen use efficiency and irrigation water productivity in rice, Field Crop. Res., 215, 1–11, https://doi.org/10.1016/j.fcr.2017.09.034, 2018.

Zhang, H., Liu, H., Hou, D., Zhou, Y., Liu, M., Wang, Z., Liu, L., Gu, J., and Yang, J.: The effect of integrative crop management on root growth and methane emission of paddy rice, Crop J., 7, 444–457, https://doi.org/10.1016/j.cj.2018.12.011, 2019.